



Mechanisms of the Molecular Mobility of Water

A. Geiger*, M. Kleene, D. Paschek, A. Rehtanz

*Physikalische Chemie, Universität Dortmund
D-44221 Dortmund, Germany*

Abstract

Based on the results of molecular dynamics simulations, mechanisms which determine the molecular mobility of water in different temperature intervals are discussed. At ambient temperature it is the intermediate formation of bifurcated H-bonds. In the supercooled liquid an approach to structural arrest is observed, which is overcome at lower temperatures by a jump diffusion mechanism. In the nearly perfect tetrahedral H-bond network of the superviscous liquid close to the glass transition temperature the occupation of interstitial positions is suggested by analogy to the observed dynamics in crystalline ice.

© 2003 Elsevier Science B.V. All rights reserved.

1 Introduction

In this review we discuss mechanisms, which govern the translational and rotational single-particle dynamics of water molecules in a wide temperature range from ambient temperatures and above to the deeply supercooled region. In the spirit of O. Samoilow [1], we intend to give here a graphical picture of the molecular processes. For more formal approaches, based on the energy landscape paradigm or the mode coupling theory, we refer to recent reviews [2,3]. Three major puzzles of the water dynamics are: Why is water so fluid, despite the fact that its hydrogen bonds form at any instance a space filling, quasi infinite network of bonds with strengths appreciably larger than the thermal energy $k_B T$ [4–7]? What are the reasons for the strong deviation from the Arrhenius law at low temperatures, leading to an apparent diverging

* Corresponding author. Fax: +49-231-755-3937

Email address: geiger@pc2a.chemie.uni-dortmund.de (A. Geiger).

Key words: Water, Molecular Dynamics, Supercooled Liquids, Glass Transition

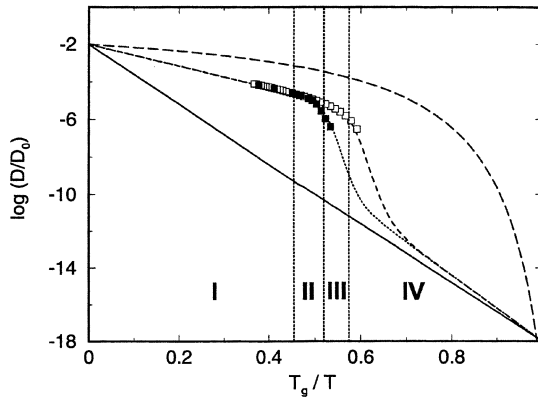


Fig. 1. Temperature dependence of the self diffusion coefficient of water. Schematic representation according to the proposition of Angell et al. [11]. Open squares: experimental [15], full squares: simulation results [16]. The roman numbers indicate the regions of different mechanisms which dominate the molecular mobility, as discussed in the text.

behaviour far above the glass transition temperature of water [8–10]? How could we understand the conjectured fragile to strong transition of the dynamic behaviour, represented schematically in the scaled Arrhenius representation ('Angell plot') of Fig.1 [11]? In this context we may also ask about possible connections to the dynamical behaviour of water in the hydration shell of hydrophobic particles and structure breaking ions [12–14].

Closely related with the dynamical behaviour are the structural and thermodynamic properties of water, especially in the metastable supercooled liquid. To explain the increasingly anomalous behaviour of water with increasing supercooling, several scenarios are discussed [17]. Based on molecular dynamics simulations, it was proposed that the anomalies of water are related to the existence of a metastable critical point in the deeply supercooled region [18,19]. Furthermore it was suggested that the polyamorphism, which is manifested by the occurrence of an apparent first order transition between a low and a high density form of amorphous ice is due to the existence of a liquid-liquid equilibrium line, extending from this second critical point into the glassy regime [20–22].

Fig.1 gives a schematic representation of the temperature dependence of the diffusion coefficient of water vs. T_g/T as suggested by Angell et al. [11]. $T_g = 136$ K is the glass transition temperature of water [23]. Due to a strong translation/rotation coupling, the same dependence holds for the inverse molecular reorientation times. We subdivide this wide temperature range into four intervals with different temperature behaviour of the single-particle

dynamic properties: At high temperatures we have an approximate Arrhenius like behaviour with low activation energy (about 20 kJ/mol at 300 K [24]); at the freezing temperature and below, the deviations from the Arrhenius line increase and can be approximated by a power law behaviour. Before the final divergence, a new mechanism is beginning to dominate, leading to a new Arrhenius like line with big slope; and finally a more weakly activated Arrhenius behaviour is expected, until the glass transition temperature is reached. It should be noted here, that the temperature dependence in the three higher temperature intervals are well studied by experiments and simulations, whereas the assumed Arrhenius behaviour in the lowest temperature interval is presently under strong debate [23]. Moreover, it is still not clear whether there is a continuity of metastable states connecting liquid water to the glass transition temperature at 136 K, or whether there is a thermodynamic discontinuity [25,26]. But this does not affect the validity of the following discussion.

In the following, we refer mainly to results from molecular dynamics simulations, which use the so called ST2 pair potential [16,27]. This potential is able to reproduce qualitatively all the anomalies of water, including the hydration effects [12,13,18]. For a more quantitative comparison with real water, it has to be kept in mind that the phase diagram of ST2 water is shifted roughly by 35 K and 80 MPa [18,28].

2 Molecular Mobility and Hydrogen Bond Network Defects

Despite the extensive association of water molecules by a spanning, quasi-infinite hydrogen-bond network well above its percolation threshold [4,5], the single particle mobility in pure water is comparable to that in simple non-associated liquids. Computer simulation studies explain this phenomenon by the existence of defects in the random tetrahedral network of hydrogen-bonds. These defects provide lower energy pathways for reorientational motions and thus 'catalyse' the restructuring of the infinitely connected network.

The basic observations, leading to the network defect picture, have been made from simulations of stretched water [29,30]. There it was observed that the mobility, i.e. the translational and rotational diffusion of water molecules decreases when the density is decreased; and in parallel the structure of the liquid changes such that an approach to a more perfect tetrahedral hydrogen-bond network can be seen. This is in contrast to the expected behaviour of normal liquids: the expansion of a sample increases the mobility due to the increase of the free volume and simultaneously the liquid becomes less structured, expressed for example by a decreasing peak height of the pair distribution functions.

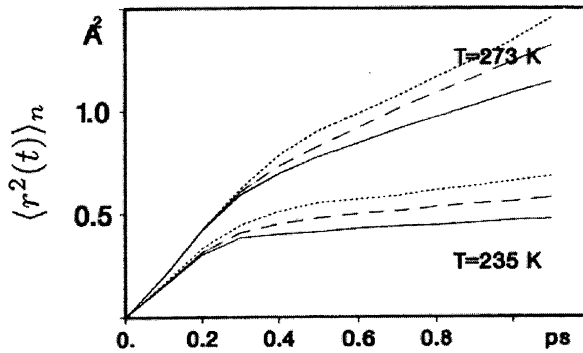


Fig. 2. Mean square displacement $\langle r^2(t) \rangle_n$ of molecules with numbers of neighbors equal to four (full line), five (dashed line) and six (dotted line) for $T = 235$ K and $T = 273$ K (from Ref. [7]).

The emergence of a more perfect tetrahedral network with decreasing density can be established by various statistical features [6,7,29,31]: the average number of nearest neighbours approaches the ice value of four; the radial distribution functions become sharper; the fraction of water molecules with more than four hydrogen-bonds, i.e. with at least one bifurcated H-bond decreases drastically; the Voronoi analysis indicates an approach to the local geometric arrangements of a perfect tetrahedral random network, as represented by the so called Polk model [31].

Simulation studies indicated a direct relation between the local deviations from the tetrahedrality ('defects'), as discussed above, and the mobility of the individual molecules. For example, it has been shown that on average the mean square displacement of molecules with more than four neighbours is increased compared to those with exactly four neighbours (Fig.2). A possible mechanism for the accelerating effect of an additional neighbour has been found, when considering the pair interaction energy V_{ij} between neighbouring molecules. In Fig.3 the corresponding distributions are given separately for two kinds of neighbouring pairs: for pairs that are connected by a linear (although possibly strongly distorted) hydrogen bond and for pairs that are connected via a bifurcated hydrogen bond (for the exact definitions see Ref. [32]). Clearly, a bifurcated bond is a network defect in the above given sense.

It is interesting to note that the distributions in Fig.3 peak at roughly -20 and -10 kJ/mol, suggesting that the sum of the two interaction energies of a bifurcated bond arrangement is roughly the energy of one linear bond. Thus a comparatively small activation energy can be sufficient to transfer one strong linear bond to another strong linear bond via the intermediate formation of a bifurcated bond, if the presence of an extra neighbour allows this. In other

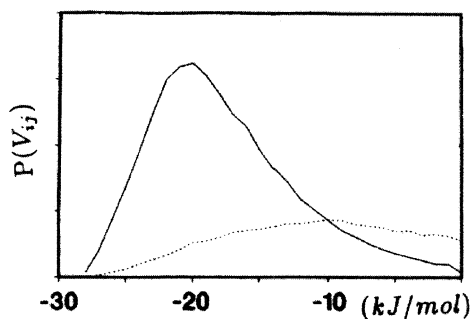


Fig. 3. Distribution function for the pair interaction energy V_{ij} for linear bonded pairs (solid line) and for pairs that are connected via a bifurcated bond (dashed line). Reproduced from Ref. [32].

words: the presence of a fifth water neighbour 'catalyses' the local reorganisation of the H-bond network. More generally, a moderate decrease of the local concentration of 'hydrogen bonding possibilities' decreases the mobility of the water molecules due to a reduction of H-bond switching possibilities. Vice versa, a concentration increase raises the molecular mobility.

These local concentration changes can not only be produced by global density changes (applying positive or negative pressures), but also locally, by dissolving other molecules. In the case of hydrophobic particles, the water molecules in the first hydration shell experience less water neighbours than in the bulk and are therefore less mobile [12,33] (the inert particle prevents the hydration shell water molecules from an approach of a fifth water neighbour). The opposite effect, where a dissolved molecule offers extra H-bond possibilities and thus increases the water mobility has been demonstrated experimentally by Kaatze and Pottel, who found a proportionality between the dielectric relaxation rates of mixtures of hydrogen bonded liquids and the spatial density of H-bond forming molecular groups [34]; and in MD simulations of aqueous solutions [30,35].

3 Structural Arrest

In supercooled water, the experimental data indicate a diverging behaviour of thermodynamic and dynamic properties at a temperature $T = 223$ K, which can be described by a power law [8–10,36]. In a series of papers, Sciortino and coworkers interpreted the apparent divergence of the dynamics as being due to a kinetic glass transition, predicted by the idealised mode coupling theory

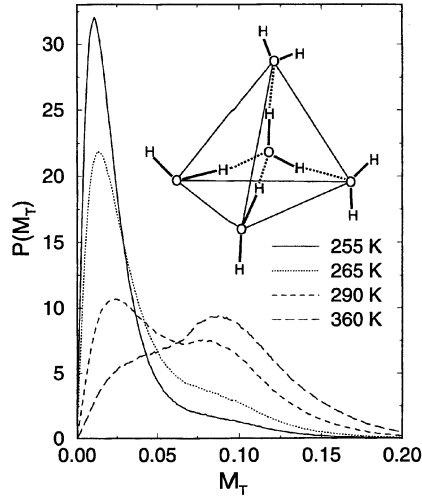


Fig. 4. Distribution of the tetrahedrality measure M_T , suggesting a temperature-dependent coexistence of two distinguishable types of local water structure [16].

[3,37,38].

According to this theory, the time evolution of various single-particle time correlation functions is characterised by a fast initial relaxation toward a plateau region, which is followed by a slow, stretched exponential decay to zero at much later times [3,38]. The extension of this plateau with decreasing temperature leads to the observed apparent divergence of transport coefficients and is due to the formation of long-lived cages around each water molecule. In contrast to simple liquids, these cages, which produce the so called 'structural arrest' are not due to a close packing, but to the formation of an ice-like tetrahedral coordination by the nearest neighbours. To illustrate this behaviour, Fig.4 shows the probability distribution of the so called 'tetrahedrality measure' M_T [39], obtained from an MD simulation of supercooled water, using the ST2 potential [16].

$$M_T = \frac{\sum_{i>j} (l_i - l_j)^2}{15 \langle l^2 \rangle} \quad (1)$$

where the l_i are the lengths of the six edges of the tetrahedron formed by the four nearest neighbours of the considered water molecule. For an ideal tetrahedron, M_T is zero. At intermediate temperatures, a bimodal distribution indicates two 'species' of water molecules: those with strongly distorted and those with a nearly perfect tetrahedral local order.

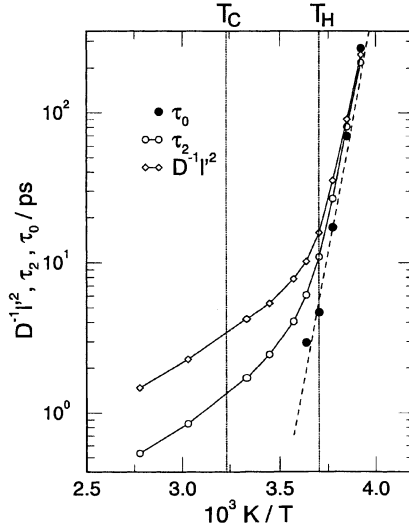


Fig. 5. Comparison of the mean residence time τ_0 with the O-H-vector reorientation time τ_2 and self diffusion coefficient D from the simulation Ref [16]. D^{-1} is multiplied by $l^2 = 1 \text{ \AA}^2$. The dashed Arrhenius line corresponds to an activation energy $E_a = 115 \text{ kJ/mol}$.

The increased formation of the tetrahedral cages at the equilibrium freezing temperature T_c and below leads to a strong increase of the reorientation time τ_2 and a corresponding decrease of the self diffusion coefficient D (see Fig.5 with results from ref. [16], the vertical line at $T_c = 310 \text{ K}$ gives the freezing temperature for the ST2 model [28])). For real water, the lowest experimentally accessible temperature is given by the homogeneous nucleation limit T_H of about 235 K . In Fig.5 this temperature (shifted by $+35 \text{ K}$, as noted above) is also indicated by a vertical line. The simulations, which can be extended beyond this limit, show that the occurrence of a perfect structural arrest, as suggested by the experimental data in the temperature range above T_H , is finally overcome by a new diffusion mechanism. This leads to a new Arrhenius-like behaviour in the lower temperature interval.

4 Jump diffusion

To make a closer connection between this new Arrhenius temperature dependence of the dynamic properties and the onset of jump diffusion, we further discuss Fig.5. Here, the reorientation times τ_2 and inverse diffusion coefficients D^{-1} are compared with the jump times τ_0 . This τ_0 has been obtained from the incoherent dynamic structure factor $S(q, \omega)$ of the center of mass motion of the

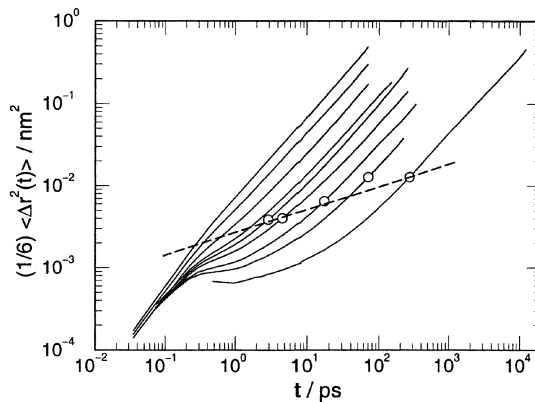


Fig. 6. Log-log plot of the center-of-mass mean square displacement for temperatures (from right to left) 255, 260, 265, 270, 275, 280, 300 and 360 K. The circles represent the jump times τ_0 from Fig.5 [16].

water molecules, by fitting a jump diffusion expression [16]. At temperatures above 275 K, τ_0 rapidly falls below 1ps. For shorter values of this quantity it is hard to speak of jump diffusion; rather a micro-step diffusion picture seems to be appropriate there. For longer residence times, all dynamic properties in Fig.5 run in parallel, revealing the dominant influence of the jump process on translation and rotation. The activation energy in this region is estimated to 115 kJ/mol, a value about 4 times the energy of a strong linear hydrogen bond.

Fig.6 substantiates the physical significance of the values for τ_0 , obtained from the fitting of $S(q, \omega)$. It shows the center of mass mean square displacement of the water molecules in log-log scale. At each temperature, the displacement at the τ_0 value from Fig.5 is marked. As can be seen, τ_0 corresponds to the time when the linear Einstein relation for the mean square displacement starts to be valid. For earlier times, the structural arrest due to the cage effect, discussed before, is evolving. Above 275 K no such cage effect can be detected.

A direct look at the molecular trajectories also supports the jump diffusion picture. In Fig.7, the trajectory of a single molecule taken from the 260 K run is depicted. The location of the oxygen atom is displayed by a closed line, while the position of the hydrogen atoms are represented by dots. A run of 844 ps length is shown. The jump-like motion becomes evident by revealing several clearly distinguishable regions of residence. The size of the depicted cube is 1 nm, so it has to be noted that some of the jumps extend to several angstroms. There is certainly a cooperative rearrangement of the surrounding hydrogen bond network necessary to enable molecules to perform such long jumps

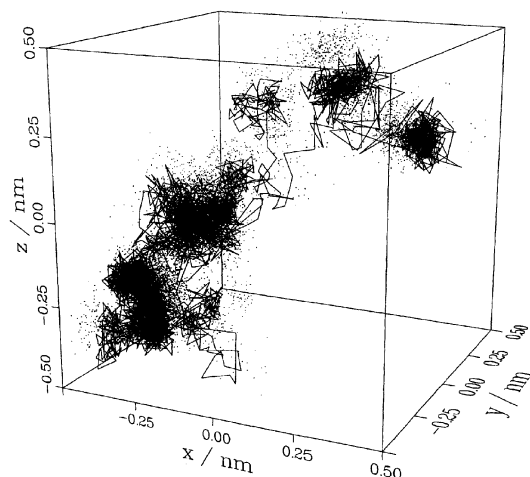


Fig. 7. Trajectory of a single molecule taken from the 260 K simulation run. The line represents the oxygen path. The hydrogen positions are represented by dots [16].

As we discussed in the previous section, an increased concentration of hydrogen bonding possibilities promotes the restructuring of the hydrogen bond network. The jump process may thus be correlated to fluctuations of the local density of the surrounding hydrogen bond donor or acceptor sites. This becomes evident from monitoring the number of nearest neighbours of a jumping particle. In Fig.8 such an event taken from the lowest temperature run is monitored. It strongly suggests that the jumps are correlated to the appearance of a fifth neighbour in the vicinity of the jumping particle.

5 Defect dynamics in ultraviscous water

The conjectured temperature dependence of Fig.1 suggests that in the temperature range close to T_g , where water must have a very high viscosity, another mechanism with lower activation energy must become prevailing, because the jump diffusion discussed in the previous section becomes extremely slow. Unfortunately, this very slow dynamics can not be accessed by computer simulations directly. But here we can discuss some hints for a possible diffusion mechanism. A justification for this far extrapolation from the temperature of our simulated system to the region of the glass transition temperature is given by the fact that no further qualitative structural changes have to be expected on further supercooling the simulated systems: the structure which has been reached at the lowest simulated temperature (see Fig.9), is already very close

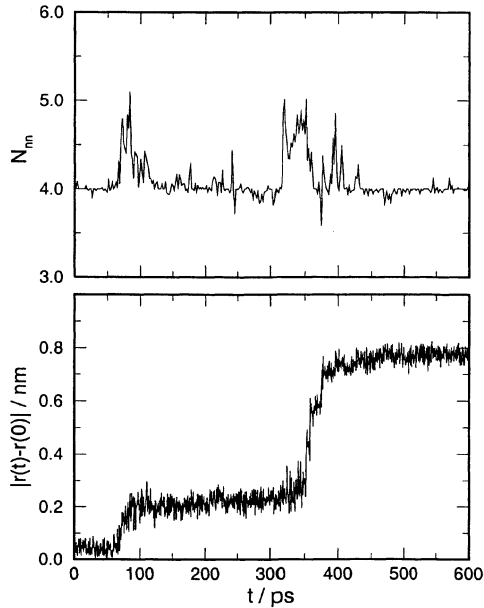


Fig. 8. Change of the local environment of a jumping particle, suggesting that the appearance of a fifth neighbor and the occurrence of the jumps are correlated: (a): Number of nearest neighbors of a selected molecule. (b): displacement of the center of mass of the same molecule [16].

to the structure of the low density amorphous ice [40,41]. Also, in the temperature range around 270 K (which would correspond to 235 K in real water), a strong decrease of the density has been observed in the simulated isobar [16]. This is in accordance with the suggested *PVT*-diagram of Mishima, when approaching the low density amorphous ice state [22].

The structural changes can best be described as an approach to a perfect tetrahedral network, comparable to the Polk model [31]. This is illustrated by Fig.10. In this Figure, sections through a large simulation box of 5822 ST2 water molecules are shown. In these snapshots the water molecules are drawn as tetrapods, the light ones represent molecules with good tetrahedral local order ($M_T < 0.06$), whereas the dark molecules have no pronounced tetrahedral surrounding ($M_T > 0.06$). A similar analysis has been presented before by Naberukhin et al. [42].

At the lowest temperature a nearly perfect tetrahedral network has formed,

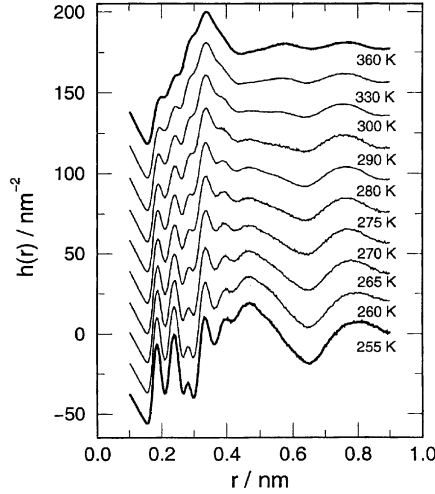


Fig. 9. $h(r) = 4\pi\rho r [0.092g_{OO}(r) + 0.486g_{HH}(r) + 0.422g_{OH}(r) - 1]$ radial distribution function to compare simulation data [16] with neutron scattering results for D₂O [40,41]. At low temperatures, the low density amorphous ice structure is approached.

with only few isolated defects. At the highest temperature the structure is nearly reversed: The regions with strongly disturbed local tetrahedrality dominate, but large patches of high local order are present. In between, a clear transition from the tetrahedral low density amorphous ice structure to the high density form of the normal liquid water is visible.

To characterise the lifetime resp. the conversion rate between the two species, we calculate time correlation functions

$$C_x(t) = \frac{\langle x(t_0)x(t_0+t) \rangle - \langle x(t_0) \rangle^2}{\langle x(t_0)^2 \rangle - \langle x(t_0) \rangle^2} \quad (2)$$

of two different dynamic properties: the time dependent tetrahedrality measure $M_T(t)$ and the characteristic two-state-function (population function)

$$\begin{aligned} F(t) &= 0, \quad \text{when } M_T(t) \geq 0.06 \\ &= 1, \quad \text{when } M_T(t) < 0.06. \end{aligned} \quad (3)$$

The pointed brackets indicate averaging over all water molecules as well as over different starting points t_0 . The time correlation functions of both quantities show the same general behaviour: after a fast initial decay a slow exponential decrease is following (see Fig.11). From the slow decay we get the relaxation times τ_M resp. τ_F for the two dynamic properties. Both coincide within the

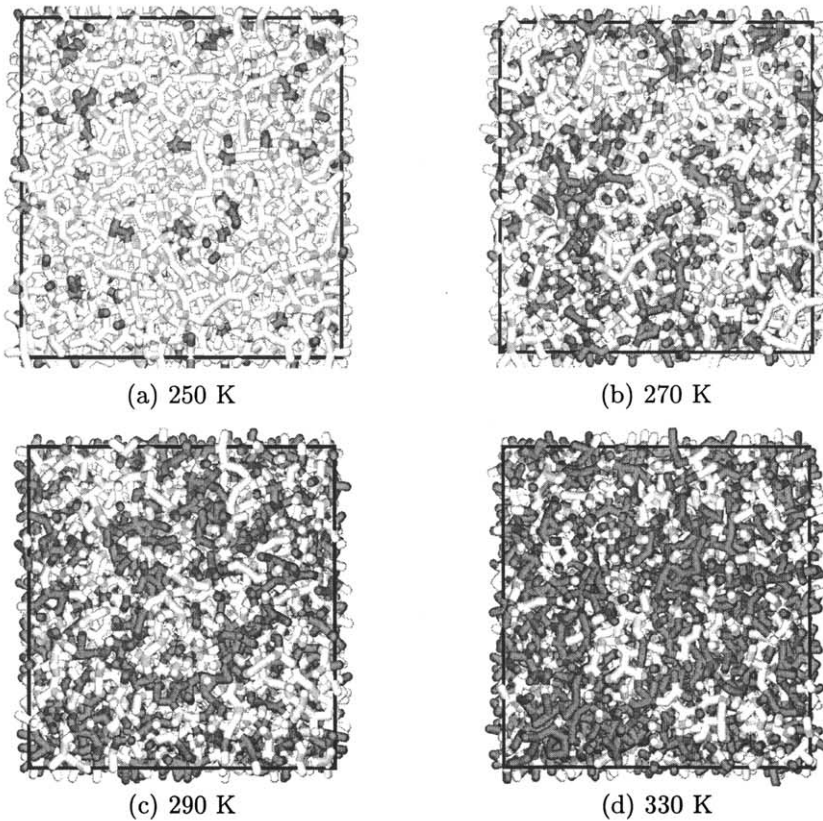


Fig. 10. Screenshots of a large simulation box at different temperatures. Molecules with good tetrahedral local order are depicted in white. At the lowest temperature a nearly perfect tetrahedral network with few local defects is formed.

statistical accuracy. The temperature dependence of τ_F is given in the insert of Fig.11 as an Arrhenius plot. The activation energy E_a is about 57 kJ/mol, a value which is intermediate between the activation energies of the two higher temperature Arrhenius regions, and above the slope of the 'ideally strong' Arrhenius line of 42 kJ/mol [23]. This is in accord with the expectations for the lowest temperature region in Fig.1. For comparison, the activation energy of the diffusion of water molecules in bulk crystalline ice is slightly higher, at 70 kJ/mol [43].

A possible molecular mechanism, which could be responsible for the diffusion dynamics in a nearly perfect tetrahedral H-bond network has been detected in an MD study of superheated ice- I_h [28]. There it was found that the most frequently occurring defect is of Frenkel type. As illustrated in Fig.12, three

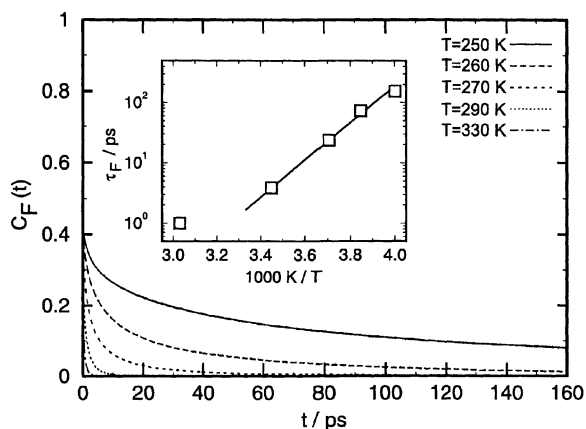


Fig. 11. Time correlation function of the tetrahedrality population function eq. 3. Insert: temperature dependence of the tail decay time τ_F .

H-bonds, marked 1 to 3, of the neighbouring water molecules *A* and *B* are broken simultaneously. The two molecules then leave their lattice sites, occupy adjacent octahedral voids in the lattice and form a new H-bond. By this, two neighbouring six-rings are transformed to two linked five-membered rings. It is quite obvious that by this move the nearly perfect tetrahedral local order of the water molecules with low M_T is transferred to a distorted one with higher M_T .

From the occurrence frequency of these defects at different temperatures, an

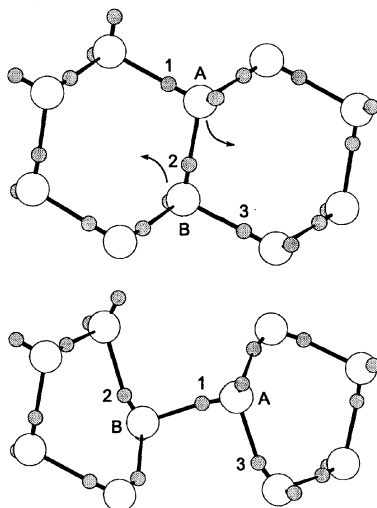


Fig. 12. Formation of a Frenkel type defect pair in an ice I_h crystal. Molecules *A* and *B* move to neighboring interstitial positions. Hydrogens 1 to 3 belong to broken and reformed H-bonds.

activation energy of about 56 kJ/mol could be estimated. This value (a) coincides with the activation energy of 57 kJ/mol, obtained for the transformation between low and high M_T molecules in the supercooled liquid, and (b) corresponds roughly to the energy necessary for the breaking of three H-bonds. Moreover, in the MD study of superheated ice, a few events could be observed, where two such steps in sequence led to a translational diffusion step in the superheated ice lattice: in partial reversal of the formation of the five-membered rings, by a similar next step A and B jump to the now unoccupied original lattice sites of each other, thus completing an interchange between A and B , the basic diffusion step in a tetrahedral lattice [28].

6 Conclusions

We have shown that at ambient temperatures it is possible to explain different observations, concerning the mobility of water molecules in aqueous systems by one simple principle: the mobility of water molecules is a function of the local density of H-bonding possibilities. The underlying mechanism is the formation of bifurcated bonds that 'catalyse' the local restructuring of the H-bond network. From this, we understand the reduction of the mobility in stretched water and in hydrophobic hydration shells, as well as the increased mobility in compressed water and in certain hydrophilic associations as local density effects.

With decreasing temperature, the local structure becomes more and more tetrahedral (ice-like). By this, a structural arrest is approached, as described by the idealised mode coupling theory. But before the total arrest is reached, the remaining thermal energy produces occasional jumps out of the cage. The resulting jump diffusion shows a high activation energy, which corresponds to the simultaneous breaking of four strong hydrogen bonds.

At even lower temperatures, when the nearly perfect tetrahedral H-bond network of the 'strong', highly viscous glass forming liquid has been formed, processes with a lower activation energy need are starting to dominate: in analogy to observations of the dynamics in superheated ice lattices, we conclude that by the intermediate formation of Frenkel-like interstitial molecules, an exchange of two water molecules can occur, thus providing a fundamental step for molecular diffusion.

References

- [1] O.J. Samoilow, *Die Struktur wässriger Elektrolytlösungen und die Hydratation von Ionen*, Teubner, Leipzig, 1961, translated from O.Ya. Samoilow, *Struktura vodnykh rastvorov elektrolitov i gidratacija iono*, Moscwa 1957.
- [2] P.G. Debenedetti, F.H. Stillinger, *Nature* 410 (2001) 259.
- [3] F. Sciortino, *Chem. Phys.* 258 (2000) 307.
- [4] A. Geiger, F.H. Stillinger, A. Rahman, *J. Chem. Phys.* 70 (1979) 4185.
- [5] R.L. Blumberg, H.E. Stanley, A. Geiger, P. Mausbach, *J. Chem. Phys.* 80 (1984) 5230.
- [6] F. Sciortino, A. Geiger, H.E. Stanley, *Nature* 354 (1991) 218.
- [7] F. Sciortino, A. Geiger, H.E. Stanley, *J. Chem. Phys.* 96 (1992) 3857.
- [8] C.A. Angell, in: F. Franks (Ed.), *Water: A Comprehensive Treatise*, Vol. 7, Plenum Press, New York, 1980, pp. 1–81.
- [9] E.W. Lang, H.D. Lüdemann, *Ber. Bunsenges. Phys. Chem.* 85 (1981) 603.
- [10] F.X. Prielmeier, E.W. Lang, R.J. Speedy, H.D. Lüdemann, *Ber. Bunsenges. Phys. Chem.* 92 (1988) 1111.
- [11] C.A. Angell, R.D. Bressel, M. Hemmati, E.J. Sare, J.C. Tucker, *Phys. Chem. Chem. Phys.* 2 (2000) 1559; C.A. Angell, C.T. Moynihan, M. Hemmati, *J. Non-Cryst. Solids.* 274 (2000) 319.
- [12] A. Geiger, A. Rahman, F.H. Stillinger, *J. Chem. Phys.* 70 (1979) 263.
- [13] A. Geiger, *Ber. Bunsenges. Phys. Chem.* 85 (1981) 52.
- [14] N.A. Chumaevski, M.N. Rodnikova, *J. Molec. Liq.* 96 (2002) 31.
- [15] K.T. Gillen, D.C. Douglas, M.J.R. Hoch, *J. Chem. Phys.* 57 (1972) 5117.
- [16] D. Paschek, A. Geiger, *J. Chem. Phys. B* 103 (1999) 4139.
- [17] P.G. Debenedetti, *Metastable Liquids*, Princeton University Press, Princeton, 1996.
- [18] P.H. Poole, F. Sciortino, U. Essmann, H.E. Stanley, *Nature* 360 (1992) 324.
- [19] H.E. Stanley, C.A. Angell, U. Essmann, M. Hemmati, P.H. Poole, F. Sciortino, *Physica A* 205 (1994) 122.
- [20] O. Mishima, *J. Chem. Phys.* 100 (1994) 5910.
- [21] O. Mishima, H.E. Stanley, *Nature* 396 (1998) 329.
- [22] H.E. Stanley, S.V. Buldyrev, M. Canpolat, O. Mishima, M.R. Sadr-Lahijany, A. Scala, F.W. Starr, *Phys. Chem. Chem. Phys.* 2 (2000) 1551.

- [23] G.P. Johari, Phys. Chem. Chem. Phys. 2 (2000) 1567; G.P. Johari, J. Phys. Chem. 116 (2002) 8067.
- [24] H. Weingärtner, Z. Phys. Chem. NF 132 (1982) 129.
- [25] P.H. Poole, F. Sciortino, T. Grande, H.E. Stanley, C.A. Angell, Phys. Rev. Lett. 73 (1994) 1632.
- [26] V.P. Shpakov, P.M. Rodger, J.S. Tse, D.D. Klug, V.R. Belosludov, Phys. Rev. Lett. 88 (2002) 5502.
- [27] F.H. Stillinger, A. Rahman, J. Chem. Phys. 60 (1974) 1545.
- [28] A. Rehtanz, Molekulardynamische Simulationen zum Wasser-Eis- I_h -System, Ph.D. thesis, Universität Dortmund (2000).
- [29] A. Geiger, P. Mausbach, J. Schnitker, in: G. Neilson, J. Enderby (Eds.), Water and Aqueous Solutions, Adam Hilger, Bristol, 1986, pp. 15–30.
- [30] A. Geiger, T. Kowall, in: M.C. Bellissent-Funel, D.J. Dore (Eds.), Hydrogen Bond Networks, Kluwer, 1994, pp. 23–35.
- [31] A. Geiger, N.N. Medvedev, Yu.I. Naberukhin, Zhurnal Strukt. Khimii 33 (1992) 79, J. Struct. Chem. 33 (1992) 226.
- [32] F. Sciortino, A. Geiger, H.E. Stanley, Phys. Rev. Lett. 65 (1990) 3452.
- [33] R. Haselmeier, M. Holz, W. Marbach, H. Weingärtner, J. Phys. Chem. 99 (1995) 2243.
- [34] U. Kaatze, R. Pottel, J. Molec. Liquids 52 (1992) 181.
- [35] T. Kowall, A. Geiger, J. Phys. Chem. 98 (1994) 6216.
- [36] W.S. Price, H. Ide, Y. Arata, O. Södermann, J. Phys. Chem. A 104 (2000) 5874.
- [37] W. Götze, L. Sjögren, Rep. Prog. Phys. 55 (1992) 241.
- [38] P. Gallo, F. Sciortino, P. Tartaglia, S.H. Chen, Phys. Rev. Lett. 76 (1996) 2630.
- [39] N.N. Medvedev, Yu.I. Naberukhin, J. Non-cryst. Solids 94 (1987) 402.
- [40] M.C. Bellissent-Funel, J. Teixeira, L. Bosio, J. Chem. Phys. 87 (1987) 2231.
- [41] M.C. Bellissent-Funel, L. Bosio, J. Chem. Phys. 102 (1995) 3727.
- [42] Yu.I. Naberukhin, V.A. Luchnikov, G.G. Malenkov, E.A. Zheligovskaya, J. Struct. Chem. 38 (1997) 593.
- [43] D.E. Brown, S.M. George, J. Phys. Chem. 100 (1996) 15460.